Energy shaping of a softening Duffing oscillator using the formalism of Port-Hamiltonian Systems

Marguerite Jossic, David Roze, Thomas Hélie, Baptiste Chomette, Adrien Mamou-Mani

ENERGY SHAPING OF A SOFTENING DUFFING OSCILLATOR USING THE FORMALISM OF PORT-HAMILTONIAN SYSTEMS

Marguerite Jossic

S3AM Team
IRCAM - Institut ∂'Alembert
Université Pierre et Marie Curie
Paris, France
marguerite.jossic@ircam.fr

David Roze, Thomas Hélie *

S3AM Team
IRCAM - Université Pierre et Marie Curie
Paris, France
david.roze@ircam.fr

Baptiste Chomette

Institut ∂'Alembert - Université Pierre et Marie Curie
Paris, France

Adrien Mamou-Mani

IRCAM - Université Pierre et Marie Curie
Paris, France

ABSTRACT

This work takes place in the context of the development of an active control of instruments with geometrical nonlinearities. The study focuses on Chinese opera gongs that display a characteristic pitch glide in normal playing conditions. In the case of the *xiaoluo* gong, the fundamental mode of the instrument presents a softening behaviour (frequency glides upward when the amplitude decreases). Controlling the pitch glide requires a nonlinear model of the structure, which can be partially identified with experimental techniques that rely on the formalism of nonlinear normal modes. The fundamental nonlinear mode has been previously experimentally identified as a softening Duffing oscillator. This paper aims at performing a simulation of the control of the oscillator's pitch glide. For this purpose, the study focuses on a single-degree-of-freedom nonlinear mode described by a softening Duffing equation. This Duffing oscillator energy proves to be ill-posed - in particular, the energy becomes negative for large amplitudes of vibration, which is physically inconsistent. Then, the first step of the present study consists in redefining a new energetically well-posed model. In a second part, guaranteed-passive simulations using port-Hamiltonian formalism confirm that the new system is physically and energetically correct compared to the Duffing model. Third, the model is used for control issues in order to modify the softening or hardening behaviour of the fundamental pitch glide. Results are presented and prove the method to be relevant. Perspectives for experimental applications are finally exposed in the last section of the paper.

1. INTRODUCTION: PROBLEM STATEMENT

The Duffing equation $\alpha\ddot{x}+\kappa x+\Gamma x^3 = 0$ is commonly used as the simplest nonlinear system that models geometrical nonlinearities. However, the softening Duffing equation ($\Gamma < 0$) leads to an ill-posed problem since the energy is negative for large amplitudes of vibration. In this study, we propose to redefine a well-posed energy to overcome this issue.

Besides, the softening Duffing oscillator is quite interesting for the study of Chinese opera gongs[1] which can present either hardening or softening behaviour in standard playing conditions. Numerous studies detailed the nonlinear dynamical phenomena that occur in these instruments (internal resonances, chaos, pitch glide, harmonic distortions, etc.)[2][3][4] and their modelization (e.g. Von Karman plate model and nonlinear normal modes[5][6]). These works showed that most of these nonlinear features are the result of nonlinear interactions between vibration modes and require models with a high number of degree of freedom[7][8]. However, in the case of the pitch glide, the uni-modal approximation might be interesting: a single nonlinear mode is able to describe the dependence between the frequency and the amplitude of vibration[5]. Nonlinear normal modes are defined as invariant manifolds in phase space [6]. They are deduced from normal form theory which allows to compute an analytical nonlinear change of variables, from modal coordinates (X_p, $\dot{X}_p$) to new normal coordinates (R_p, $\dot{R}_p$), by cancelling all the terms that are not dynamically important in the equations of motion [9]. The dynamics onto the p-th nonlinear normal mode is governed by the new normal coordinates (R_p, $\dot{R}_p$) and is written in free vibration regime:

$$\ddot{R}_p + \omega_p^2 R_p + (A_p + C_p)R_p^3 + B_p R_p \dot{R}_p{}^2 = 0 \qquad (1)$$

where R_p and $\dot{R}_p$ are the nonlinear mode displacement and velocity respectively, ω_p is the modal pulsation associated with the p-th mode, and A_p, C_p and B_p are coefficients that take into account the influence of other linear modes in the nonlinear mode dynamics. A first-order perturbative development of this equation [10] leads to the nonlinear relationship between the angular frequency of nonlinear free oscillations ω_{NL} and the amplitude a of the nonlinear mode's response at frequency ω_{NL}:

$$\omega_{NL} = \omega_p(1 + T_p a^2)$$

where the coefficient T_p is $T_p = \frac{3(A_p+C_p)+\omega_p^2 B_p}{8\omega_p^2}$. In practice, an experimental identification of T_p can be performed [11], but afterwards it is no longer possible to identify separately the coefficients A_p, C_p and B_p. However, in the case of the *xiaoluo*, it can be shown that the fundamental nonlinear mode described in (1) is equivalent (first-order of perturbation method) to a softening Duffing equation with a negative cubic coefficient Γ_p:

$$\ddot{R}_p + \omega_p^2 R_p + \Gamma_p R_p^3 = 0 \qquad (2)$$

* The contribution of this author has been done at laboratory STMS, Paris, within the context of the French National Research Agency sponsored project INFIDHEM. Further information is available at http://www.lagep.cpe.fr/wwwlagep7/anr-dfg-infidhem-fev-2017-jan-2020/

Indeed, the T_p coefficient in this case is directly related to the Γ_p by $T_p = \frac{3\Gamma_p}{8\omega_p^2}$. Then, provided that:

$$\Gamma_p = A_p + C_p + \frac{\omega_p^2 B_p}{3}$$

the equation (1) is equivalent to (2). Consequently, the coefficient Γ_p and therefore the nonlinear mode can be experimentally identified with the measurement of T_p.

Finally, the softening Duffing model is assumed for two reasons: first, it provides a convenient basis to experimentally identify isolated nonlinear modes in the case of gongs; second, it gives the opportunity to define a single parameter well-posed energy that can be manipulated through energy shaping control in order to change its softening or hardening behaviour.

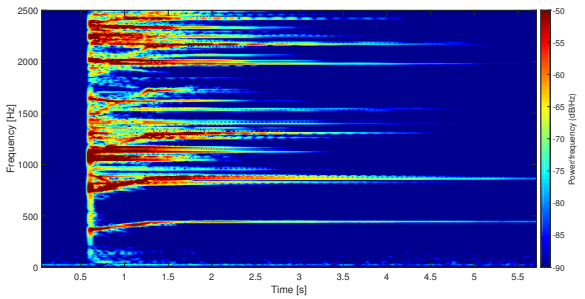

Figure 1: *Spectrogram of the sound of a xiaoluo after being struck by a mallet. The fundamental mode (∼ 449 Hz) displays a softening behaviour.*

This study aims at controlling the softening behaviour of the *xiaoluo* gong's nonlinear fundamental mode, that we assume to be a in the form of the softening Duffing equation described by Eq. (2). The control process relies on guaranteed-passive simulations that use port-Hamiltonian approach. Port-Hamiltonian systems (PHS) are an extension of Hamiltonian systems, which represent passive physical systems as an interconnection of conservative, dissipative and sources components. They provide a unified mathematical framework for the description of various physical systems. In our case, the PHS formalism allows for the writing of an energy-preserving numerical scheme [12] in order to simulate and control the Duffing equation - note that other and more precise guaranteed-passive numerical schemes [13] are available but not used in this work. The first observation when tackling the control problem is that the softening Duffing equation defined by Eq. (2) is energetically ill-defined (Section 2). For large amplitudes of vibration, the total system energy, written with the PHS approach, becomes negative and thus, physically inconsistent. The first step of this study consists then to redefine the energy for the fundamental nonlinear mode. This new energy must be (i) as close as possible of the energy of the Duffing equation described in (2) and (ii) physically consistent. Secondly (Section 3), the Duffing energy and the new well-posed energy are both simulated using a guaranteed-passive numerical scheme that relies on the energy discrete gradient. Simulation results confirm the relevance of using the new energy for the control design. Thirdly (Section 4), control simulation of the fundamental mode's pitch glide is realized by shaping the system's new energy. The simulation results confirm the ability to modify the softening behaviour of the fundamental mode thanks to the new energy defined in Section 2. Finally, conclusion and perspectives for further research offered by this study are discussed in Section 5.

2. PHYSICAL MODEL

2.1. Original Duffing model

2.1.1. Equation of motion

As explained before, the nonlinear normal mode associated with the fundamental mode is modelled by a softening Duffing oscillator, expressed as in Eq. (2) with an added viscous modal damping:

$$\ddot{x}(t) + 2\xi\omega_0\dot{x}(t) + \omega_0^2 x(t) - \Gamma x^3(t) = f(t) \tag{3}$$

where x is the amplitude response of the nonlinear normal mode, ξ is the modal damping factor, ω_0 is the modal pulsation, Γ is the nonlinear cubic coefficient ($\Gamma > 0$) and f is the input acceleration. These parameters have been experimentally identified, however the description of the identification methods are beyond the scope of the paper. We assume then the following parameters values:

$$\xi = 1.4.10^{-3}$$
$$\omega_0 = 2\pi \times 449 \text{ rad/s}$$
$$\Gamma = 6,7.10^{6} \text{ S.I}$$

2.1.2. Dimensionless problem

For more convenience, equation (3) is written with dimensionless amplitude $\tilde{x}$ and time $\tilde{t}$, defined such as $x = X_0\tilde{x}$ and $t = \tau\tilde{t}$. The Duffing equation (3) becomes:

$$\frac{X_0}{\tau^2}\ddot{\tilde{x}}(\tilde{t}) + 2\xi\omega_0^2\frac{X_0}{\tau}\dot{\tilde{x}}(\tilde{t}) + \omega_0^2 X_0\tilde{x}(\tilde{t}) - \Gamma X_0^3\tilde{x}^3(\tilde{t}) = f(\tau\tilde{t})$$

that is:

$$\ddot{\tilde{x}}(\tilde{t}) + 2\xi\omega_0^2\tau\dot{\tilde{x}}(\tilde{t}) + \omega_0^2\tau^2\tilde{x}(\tilde{t}) - \Gamma\tau^2 X_0^2\tilde{x}^3(\tilde{t}) = \frac{f(\tau\tilde{t})\tau^2}{X_0}$$

Choosing τ and X_0 such that $\tau = \frac{1}{\omega_0}$ and $X_0 = \sqrt{\frac{1}{\tau^2\Gamma}}$ leads to the following Duffing equation:

$$\ddot{\tilde{x}}(\tilde{t}) + \mu\dot{\tilde{x}}(\tilde{t}) + \tilde{x}(\tilde{t}) - \tilde{x}^3(\tilde{t}) = \tilde{f}(\tilde{t}) \tag{4}$$

where $\mu = 2\xi$ and $\tilde{f}(\tilde{t}) = \frac{f(\tau\tilde{t})\sqrt{\Gamma}}{\omega_0^2 m}$.

For sake of legibility, tilde will be omitted in the following.

2.2. Port-Hamiltonian approach

This section introduces some recalls on port-Hamiltonian systems in finite dimensions. The calculation of the Hamiltonian H of the Duffing system demonstrates that its potential energy H_1 is negative for some displacement values. A new equivalent positive definite potential energy $H_{1\star}$ is then defined for the control design.

2.2.1. General formulation

A port-Hamiltonian system of state $\boldsymbol{x}(t)$, input $\boldsymbol{u}(t)$ and output $\boldsymbol{y}(t)$ can be represented by the following differential equations [14]:

$$\begin{aligned}\dot{\boldsymbol{x}} &= \big(\boldsymbol{J}(\boldsymbol{x}) - \boldsymbol{R}(\boldsymbol{x})\big)\boldsymbol{\nabla}_{\boldsymbol{x}} H(\boldsymbol{x}) + \boldsymbol{G}(\boldsymbol{x})\boldsymbol{u} \\ \boldsymbol{y} &= \boldsymbol{G}(\boldsymbol{x})^T \boldsymbol{\nabla}_{\boldsymbol{x}} H(\boldsymbol{x})\end{aligned}$$

where $\dot{\boldsymbol{x}}$ is the time derivative of state $\boldsymbol{x}$, $\boldsymbol{\nabla}_{\boldsymbol{x}}$ denotes the gradient with respect to state $\boldsymbol{x}$, $H(t)$ is a positive definite function that represents the total energy of the system, matrix $\boldsymbol{J}$ is skew-symmetric and $\boldsymbol{R}$ is positive definite ($\boldsymbol{R} \geq 0$). The power balance of the system can be expressed by the temporal energy variation of the system $\dot{H}(\boldsymbol{x}(t)) = \boldsymbol{\nabla}_{\boldsymbol{x}} H(\boldsymbol{x}(t))^T \dot{\boldsymbol{x}}(t)$, that is:

$$\dot{H} = \underbrace{\boldsymbol{\nabla}_{\boldsymbol{x}} H^T \boldsymbol{J} \boldsymbol{\nabla}_{\boldsymbol{x}} H}_{=0\ (\boldsymbol{J}=-\boldsymbol{J}^T)} - \underbrace{\boldsymbol{\nabla}_{\boldsymbol{x}} H^T \boldsymbol{R} \boldsymbol{\nabla}_{\boldsymbol{x}} H}_{\text{Dissipated power } \mathcal{P}_d > 0} + \underbrace{\boldsymbol{y}^T \boldsymbol{u}}_{\text{Entering power } \mathcal{P}_e} .$$

This power balance equation guarantees the system passivity. The variation of the system energy is expressed as the sum of elementary power functions corresponding to the storage, the dissipation and the exchanges of the system with the external environment. The dissipation term $\mathcal{P}_d$ is positive because $\boldsymbol{R}$ is positive definite. The power term $\mathcal{P}_e$ denotes the energy provided to the system by the ports $\boldsymbol{u}(t)$ and $\boldsymbol{y}(t)$ (external sources).

The formulation $\dot{H}(\boldsymbol{x}) = \boldsymbol{\nabla}_{\boldsymbol{x}} H(\boldsymbol{x})^T \dot{\boldsymbol{x}}$ underlines the fact that each power function can be expressed as the product of a flux ($[\boldsymbol{\nabla}_{\boldsymbol{x}} H(\boldsymbol{x})^T]_i$ or $[\dot{\boldsymbol{x}}]_i$) with its associated efforts ($[\dot{\boldsymbol{x}}]_i$ or $[\boldsymbol{\nabla}_{\boldsymbol{x}} H(\boldsymbol{x})^T]_i$). A concrete example is given below with the Duffing oscillator described by Eq. (4) .

2.2.2. Softening Duffing oscillator energy

The port-Hamiltonian system corresponding to the Duffing equation (4) can be defined as follow:

- State: $\boldsymbol{x} = \begin{bmatrix} x_1 \\ x_2 \end{bmatrix} = \begin{bmatrix} l \\ p \end{bmatrix}$
  where l and p are the string elongation and the mass momentum, respectively.
- Dissipation: $\mathcal{P}_D = \mu p^2 > 0$.
- Source: input $u = f$ and output $-y = p$.

where p is the velocity of the nonlinear normal mode. The total energy of the system H is the sum of the energy of the spring H_1 and the energy of the mass H_2:

$$H(x_1, x_2) \quad = \quad H_1(x_1) + H_2(x_2) = \frac{1}{2}x_1^2 - \frac{1}{4}x_1^4 + \frac{1}{2}x_2^2$$

The flux and efforts associated with the energies H_1 and H_2 are given in Table 1.

	Spring	Mass
Energy	$H_1(x_1) = \frac{1}{2}x_1^2 - \frac{1}{4}x_1^4$	$H_2(x_2) = \frac{1}{2}x_2^2$
Effort	$\frac{dH_1(x_1)}{dl} = x_1 - x_1^3$	$\frac{dx_2}{dt}$
Flux	$\frac{dx_1}{dt}$	$\frac{dH_2(x_2)}{dx_2} = x_2$

Table 1: Energies and associated efforts and flux.

The port-Hamiltonian formulation of Eq. (4) can be deduced:

$$\begin{aligned}\dot{\boldsymbol{x}} &= (\boldsymbol{J} - \boldsymbol{R})\boldsymbol{\nabla}_{\boldsymbol{x}} H(\boldsymbol{x}) + \boldsymbol{G}u \\ \begin{pmatrix}\dot{x}_1 \\ \dot{x}_2\end{pmatrix} &= \left[\begin{pmatrix}0 & 1 \\ -1 & 0\end{pmatrix} - \begin{pmatrix}0 & 0 \\ 0 & \mu\end{pmatrix}\right] \boldsymbol{\nabla}_{\boldsymbol{x}} H(x_1, x_2) + \begin{pmatrix}0 \\ 1\end{pmatrix} u\end{aligned}$$

The physical interpretation of a system is often analyzed through the derivative of the potential energy (or forces), which is written in our case:

$$H_1'(x_1) = x_1 - x_1^3$$

The derivative H_1' is plotted on Figure 2(a) with the potential energy derivative of the underlying linear system for comparison. One can see that looking at H_1' does not give any information about the physical existence of the softening Duffing system. It is only by plotting the potential energy H_1 (see Figure 2(b)) that the softening system proves not to be physically defined for some displacement values x_1: if $|x_1| > \sqrt{2}$, $H_1 < 0$ and H can be negative. Moreover, the equilibrium points $x_1 = 1$ and $x_1 = -1$ are saddle points, which means that the physical problem is restricted to $|x_1| < 1$.

The softening Duffing system (4) is then not energetically defined, and a new well-posed energy needs to be sought for the control design.

2.2.3. Well-posed problem

The aim of this paper is to seek functions $H_{1\star}$ such that:

$$\begin{aligned}&\bullet\ \forall x \in \mathbb{R},\ H_{1\star}(x) \geq 0 \\ &\bullet\ H_{1\star} \text{ increases on } \mathbb{R}^+ \\ &\bullet\ H_{1\star} \text{ decreases on } \mathbb{R}^- \\ &\bullet\ H_{1\star}'' \text{ is equivalent at order 2 to the dynamical stiffness of} \\ &\quad \text{the softening Duffing } H_1''(x) = 1 - 3x^2\end{aligned} \tag{5}$$

$H_1''(x)$ corresponds to the first terms of the Taylor expansion of $x \to \exp(-3x^2)$. Then, one simple choice for $H_{1\star}''$ is:

$$\forall x \in \mathbb{R} \quad H_{1\star}''(x) = \exp(-3x^2) = \sum_{n=0}^{+\infty} \frac{(-3)^n}{n!} x^{2n}$$

If we assume the conditions $H_{1\star}'(0) = 0$ and $H_{1\star}(0) = 0$, the simple and double integration of $H_{1\star}''$ give, for all $x \in \mathbb{R}$:

$$H_{1\star}'(x) = \sum_{n=0}^{+\infty} \frac{(-3)^n}{n!(2n+1)} x^{2n+1} = x - x^3 + O(x^5)$$

$$H_{1\star}(x) = \sum_{n=0}^{+\infty} \frac{(-3)^n}{(2n+2)(2n+1)n!} x^{2n+2} = \frac{x^2}{2} - \frac{x^4}{4} + O(x^6)$$

and $H_{1\star}$ meets the requirements (5). Note that $H_{1\star}'$ can be expressed with the help of the error function erf which is defined for $x \in \mathbb{R}$ by:

$$erf(x) = \frac{2}{\sqrt{\pi}} \int_0^x e^{-\lambda^2} \mathrm{d}\lambda = \frac{2}{\sqrt{\pi}} \sum_{n=0}^{\infty} (-1)^n \frac{x^{2n+1}}{n!(2n+1)}$$

leading to:

$$H_{1\star}'(x) = \frac{\sqrt{\pi}}{2\sqrt{3}} erf(\sqrt{3}x)$$

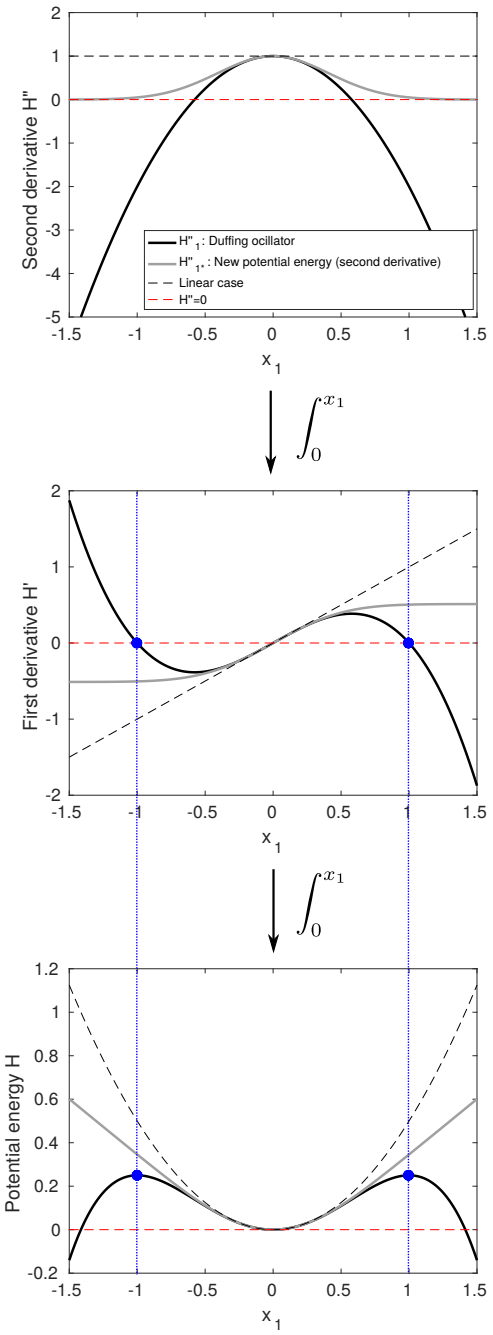

Figure 2: Second derivative, first derivative of potential energy and potential energy obtained by successive integrations with respect to the displacement x_1, represented in the case of the Duffing oscillator, the new well-posed energy, and the linear case. Red dot line represents the null energy level, and blue dot line indicates the coincidence between the turning points of the potential energy and the zeros of its first derivative.

Finally, the new potential energy is:

$$\begin{aligned} H_{1\star}(x) &= \sum_{n=0}^{+\infty} \frac{(-3)^n}{n!(2n+1)(2n+2)} x^{2n+2} \\ &= \frac{\sqrt{\pi}}{6} p(\sqrt{3}x) - \frac{1}{6} \end{aligned}$$

where $p(x) = x \times erf(x) + \frac{e^{-x^2}}{\sqrt{\pi}}$ is a primitive of the erf function. The potential energy $H_{1\star}$ and its derivative are represented in Figure 2 along with H_1 and the linear system potential energy for comparison. Note that $H_{1\star}$ is positive and equals the Duffing potential energy H_1 for small amplitudes x_1.

3. SIMULATION

This section describes the MATLAB guaranteed-passive structure simulation relying on the discrete energy gradient. The simulation of the systems defined by (i) the Duffing potential energy H_1 and (ii) the well-posed problem defined by the new potential energy $H_{1\star}$ are performed and compared.

3.1. Discretization of the equations

The discrete-time equations to be solved for the port-Hamiltonian system are:

$$\begin{cases} \frac{\delta \boldsymbol{x}}{\delta t} &= (\boldsymbol{J}(\boldsymbol{x}) - \boldsymbol{R}(\boldsymbol{x}))\boldsymbol{\nabla}_d H(\boldsymbol{x}, \delta\boldsymbol{x}) + \boldsymbol{G}(\boldsymbol{x})\boldsymbol{u} \\ \boldsymbol{y} &= \boldsymbol{G}(\boldsymbol{x})^T \boldsymbol{\nabla}_d H(\boldsymbol{x}, \delta\boldsymbol{x}) \end{cases} \quad (6)$$

where $\delta\boldsymbol{x} = [\delta x_1 \delta x_2]^T$ and δt ($\delta t = 1/f_s$ where $f_s = 44100$ Hz is the sampling frequency) are the discrete space and time step, respectively, and $\boldsymbol{\nabla}_d$ denotes the discrete gradient defined by:

$$\begin{aligned} [\boldsymbol{\nabla}_d H(\boldsymbol{x}, \delta\boldsymbol{x})]_n &= \frac{H_n(x_n + \delta x_n) - H_n(x_n)}{\delta x_n} \text{ if } \delta x_n \neq 0 \\ &= H_n'(x_n) \text{ else.} \end{aligned}$$

Matrices $\boldsymbol{J}$, $\boldsymbol{R}$ and $\boldsymbol{G}$ are defined as:

$$\boldsymbol{J} = \begin{pmatrix} 0 & 1 \\ -1 & 0 \end{pmatrix}$$
$$\boldsymbol{R} = \begin{pmatrix} 0 & 0 \\ 0 & \mu \end{pmatrix}$$
$$\boldsymbol{G} = \begin{pmatrix} 0 \\ 1 \end{pmatrix}$$

Equation (6) is implicit and requires an iterative algorithm to be solved. In this work we use the Newton-Raphson method, which is written for time step k:

$$\delta\boldsymbol{x}^{(k+1)} = \delta\boldsymbol{x}^{(k)} - \boldsymbol{J}_{\boldsymbol{F}}^{-1}(\delta\boldsymbol{x}^{(k)})\boldsymbol{F}(\delta\boldsymbol{x}^{(k)}), \quad k \in \mathbb{N}$$

where $\boldsymbol{J}_{\boldsymbol{F}}$ is the Jacobian matrix of function $\boldsymbol{F}$ defined by $\boldsymbol{F}(\delta\boldsymbol{x}) = \boldsymbol{0}$ that is:

$$\begin{aligned} \boldsymbol{F} &= \begin{pmatrix} F_1(\delta x_1, \delta x_2) \\ F_2(\delta x_1, \delta x_2) \end{pmatrix} \\ &= \frac{1}{\delta t}\begin{pmatrix} \delta x_1 \\ \delta x_2 \end{pmatrix} - \begin{pmatrix} 0 & 1 \\ -1 & -\mu \end{pmatrix}\begin{pmatrix} \nabla_d H_1(x_1, \delta x_1) \\ \nabla_d H_2(x_2, \delta x_2) \end{pmatrix} - \begin{pmatrix} 0 \\ 1 \end{pmatrix} u \end{aligned}$$

3.2. Duffing case

In the Duffing oscillator case, the discrete gradient is:

$$\begin{aligned} \nabla_d H_1(x_1, \delta x_1) &= \frac{H_1(x_1 + \delta x_1) - H_1(x_1)}{\delta x_1} \\ &= \frac{1}{2}(2x_1 + \delta x_1) - \frac{1}{4}(4x_1^3 + 6x_1^2\delta x_1 + 4x_1\delta x_1^2 + \delta x_1^3) \end{aligned} \quad (7)$$

and

$$\begin{aligned}\nabla_d H_2(x_2, \delta x_2) &= \frac{H_2(x_2+\delta x_2) - H_2(x_2)}{\delta x_2} \\ &= x_2 + \frac{\delta x_2}{2}\end{aligned}$$

Then we have:

$$\begin{aligned}F_1(\delta x_1, \delta x_2) &= \frac{\delta x_1}{\delta t} - \nabla_d H_2(x_2, \delta x_2) \\ F_2(\delta x_1, \delta x_2) &= \frac{\delta x_2}{\delta t} + \nabla_d H_1(x_1, \delta x_1) + \mu \nabla_d H_2(x_2, \delta x_2) - u\end{aligned}$$

and the Jacobian matrix is:

$$\boldsymbol{J_F} = \begin{pmatrix} \frac{1}{\delta t} & -\frac{1}{2} \\ \frac{1}{2} - \frac{3}{2}x_1^2 - 2x_1\delta x_1 - \frac{3}{4}\delta x_1^2 & \frac{1}{\delta t} + \frac{\mu}{2} \end{pmatrix}$$

The simulation of the Duffing oscillator is performed with an excitation force $f(t) = f_0 \cdot g(t)$ where g is an impulse. The potential energy H_1 versus the simulated displacement x_1, for the limit excitation $f_0 = f_{max} = 9.5 \cdot 10^7$, is plotted in Figure 3. The spectrogram of the oscillator response x_1 is also shown in Figure 4 and highlights the softening behaviour of the oscillator. If the value of f_0 exceed f_{max}, the simulation fails since $|x_1| > 1$ (see Section 2). We will see in the next section that this difficulty can be overcome with the definition of a new potential energy.

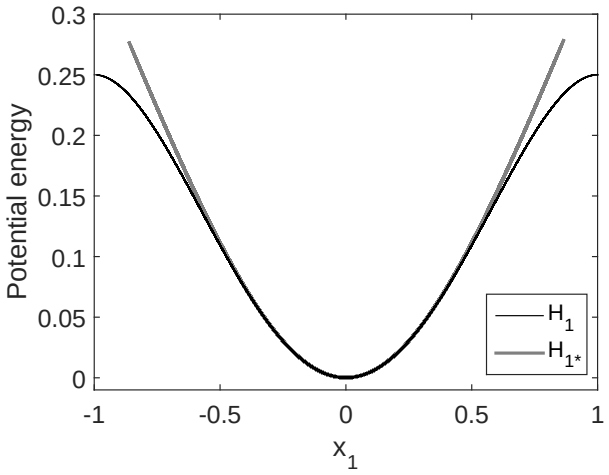

Figure 3: *Potential energies as a function of the displacement resulting from simulations of the Duffing oscillator (black) and the new well-posed model (grey). The excitation force is* $f_{max} = 9.5 \cdot 10^7$. *In the case of the Duffing oscillator, increasing the input force makes the computation fail because* $|x_1| > 1$ *(see Fig 2).*

3.3. Well-posed problem

In the case of the new problem defined by $H_{1\star}$ the discrete gradient is

$$\begin{aligned}\nabla_d H_{1\star}(x_1, \delta x_1) &= \frac{H_{1\star}(x_1+\delta x_1) - H_{1\star}(x_1)}{\delta x_1} \\ &= \frac{\sqrt{\pi}}{6} \frac{p(\sqrt{3}(x_1+\delta x_1)) - p(\sqrt{3}x_1)}{\delta x_1} \qquad (8)\end{aligned}$$

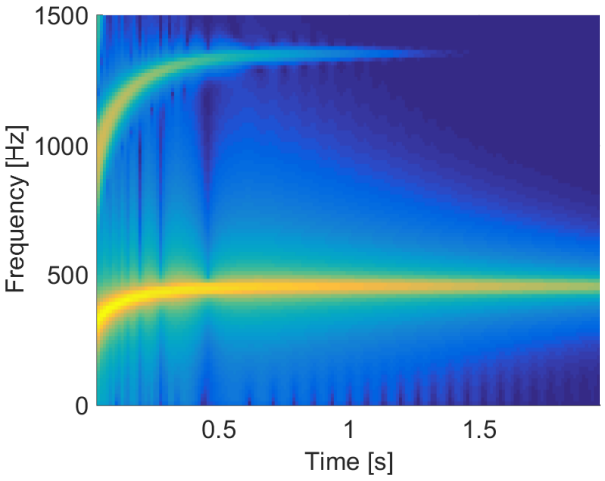

Figure 4: *Spectrogram of the simulated Duffing system response* x_1 *for an input force* $f_{max} = 9.5 \cdot 10^7$.

$\nabla_d H_2(x_2, \delta x_2)$ is the same as in the Duffing case. We can then deduce the Jacobian matrix:

$$\boldsymbol{J_F} = \begin{pmatrix} \frac{1}{\delta t} & -\frac{1}{2} \\ \frac{\sqrt{\pi}}{6} \frac{\sqrt{3}p'(\sqrt{3}(x_1+s_1))s_1 - p(\sqrt{3}(x_1+s_1)) + p(\sqrt{3}x_1)}{s_1^2} & \frac{1}{\delta t} + \frac{\mu}{2} \end{pmatrix}$$

It is possible to simulate the system associated with the new energy $H_{1\star}$ for an excitation force $f_0 = f_{max}$, as in section 3.2. The potential energy $H_{1\star}$ versus the simulated displacement is plotted in Figure 3 and can be compared with the potential energy issued from the Duffing simulation performed in section 3.2. However, contrary to the Duffing simulation, the input force f_0 can now be increased without failing the computation. This is demonstrated by running simulations with an input force $f_0 = 2 \cdot 10^8 > f_{max}$. The resulting potential energy $H_{1\star}$ is plotted in Figure 5 and the spectrogram of the temporal displacement x_1 is represented in Figure 6: the softening behaviour of the system has been increased.

4. CONTROL DESIGN

In this section, we present the nonlinear mode's pitch glide control design. The former Duffing model presented in Section 2 is abandoned and replaced by the model associated with the new potential energy $H_{1\star}$ defined in Section 3. The control of the pitch glide is realized by shaping the energy $H_{1\star}$. The principles of energy shaping are recalled in the first section, and the pitch glide control simulations are presented in the second section.

4.1. Energy reshaping

Let $H_{1\star}^{\epsilon}$ be the potential energy parameterized by $\epsilon \neq 0$ such that:

$$H_{1\star}^{\epsilon}(x) = \frac{x^2}{2} - \epsilon\frac{x^4}{4} + O(x^6) \qquad (9)$$

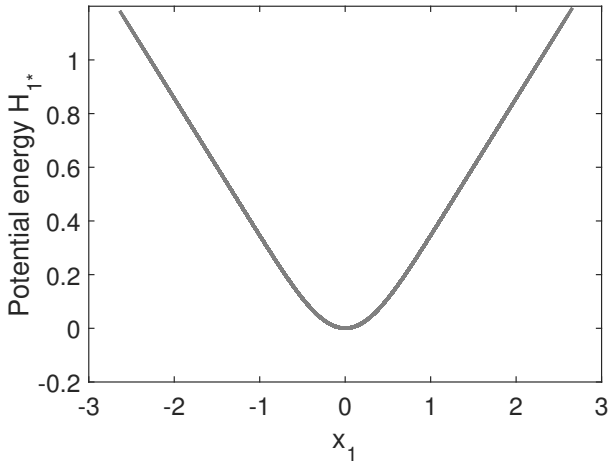

Figure 5: *Potential energy H_{1*} as a function of the displacement x_1 resulting from simulations of the new well-posed system for an input force $f_0 = 2 \cdot 10^8 > f_{max} = 9.5 \cdot 10^7$.*

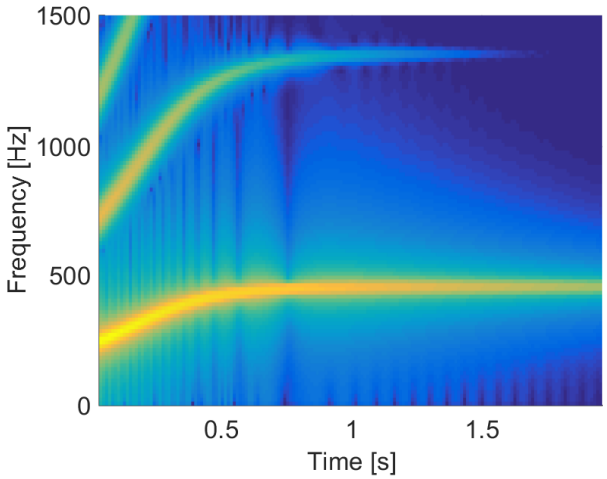

Figure 6: *Spectrogram of the simulated well-posed system response x_1 for an input force $f_0 = 2 \cdot 10^8 > f_{max} = 9.5 \cdot 10^7$.*

This potential energy can be easily calculated using the same arguments than in section 2.2.3:

$$H^{\epsilon}_{1\star}(x) = \frac{\sqrt{\pi}}{6\epsilon} p(\sqrt{3\epsilon}x) - \frac{1}{6\epsilon} \quad \text{for } \epsilon > 0 \quad \text{(softening)}$$

$$H^{\epsilon}_{1\star}(x) = \frac{\sqrt{\pi}}{6\epsilon} p_i(\sqrt{3\epsilon}x) + \frac{1}{6\epsilon} \quad \text{for } \epsilon < 0 \quad \text{(hardening)}$$

where $p_i(x) = x \times erfi(x) - \frac{e^{x^2}}{\sqrt{\pi}}$ is a primitive of the imaginary error function $erfi$.

The energy shaping control principle is as follows: if a system is defined by the energy $H^{\epsilon_1}_{1\star}$, energy shaping consists in changing the system potential energy from $H^{\epsilon_1}_{1\star}$ to $H^{\epsilon_2}_{1\star}$ ($\epsilon_1 \neq \epsilon_2$) by replacing at each time step t the input force $f(t)$ by:

$$f_1(t) = f(t) + (\nabla_d H_1^{\epsilon_1} - \nabla_d H^{\epsilon_2}_{1\star})(x_1(t))$$

The gradient term $+\nabla_d H_1^{\epsilon_1}$ aims at "cancelling" the original system defined by $H^{\epsilon_1}_{1\star}$ whereas the gradient term $-\nabla_d H^{\epsilon_2}_{1\star}$ introduces the new target system defined by $H^{\epsilon_2}_{1\star}$. In our case, note that the original system is defined by $\nabla_d H_{1\star} = \nabla_d H^{\epsilon_1=1}_{1\star}$.

4.2. Control simulations

Control simulations using energy shaping principle are performed. The simulation parameters are:

- initial (uncontrolled) energy: $H^{\epsilon_1}_{1\star} = H_{1\star}$
- target energy: $H^{\epsilon_2}_{1\star}$, with $\epsilon_2 \in \{0.0746, 0.746, 1.79, -2\}$
- input force: $f_0 = 2 \cdot 10^8$

Note that $\epsilon_2 > 0$ and $\epsilon_2 < 0$ leads to a softening and hardening behaviour, respectively.

Figure 7 presents the potential energy $H^{\epsilon_2}_{1\star}$ computed from the simulated responses for the different values of ϵ_2. Theoretical quadratic energy of the underlying linear system is also plotted to distinguish softening from hardening behaviour. The results show that positive control parameter ϵ_2 leads to a softening behaviour (which increases with the value of ϵ_2), whereas negative value of ϵ_2 results in a hardening behaviour, as expected. This is confirmed by looking at the pitch glide variation of the system response, in Figure 8 to 11.

These results underline the benefits of the definition of the new energy $H_{1\star}$, i.e. the ability to compute systems dynamics with important pitch glide (downward and upward) caused by both large input forces and nonlinear coefficients.

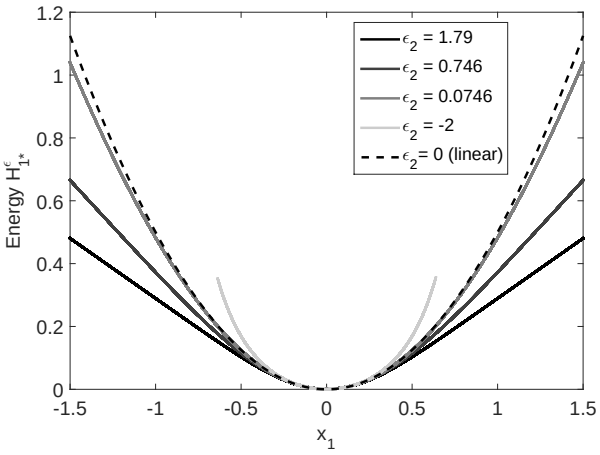

Figure 7: *$H^{\epsilon}_{1\star}$ energies of the controlled system for different values of control parameter ϵ_2.*

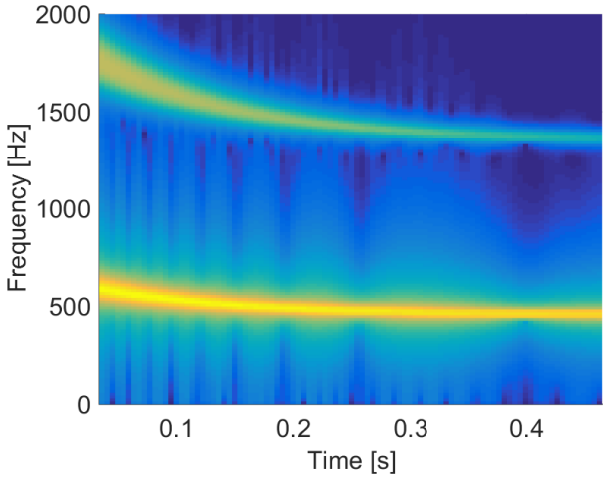

Figure 8: *Spectrogram of the system response x_1 for a control parameter value $\epsilon_2 = -2$.*

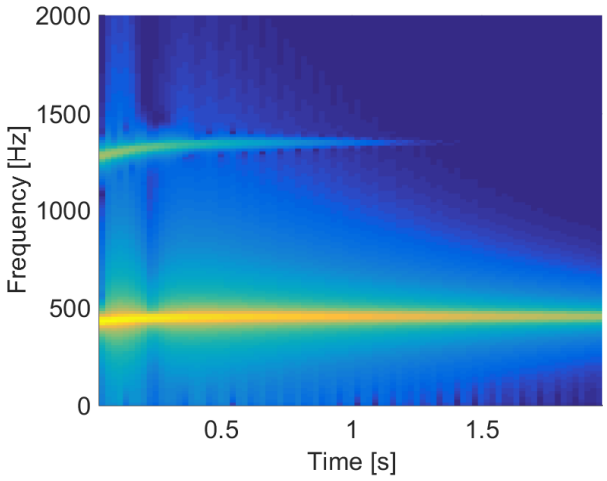

Figure 9: *Spectrogram of the system response x_1 for a control parameter value $\epsilon_2 = 0.0746$*

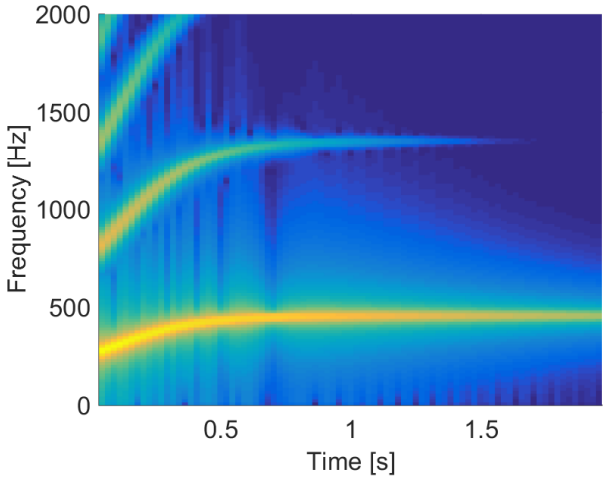

Figure 10: *Spectrogram of the system response x_1 for a control parameter value $\epsilon_2 = 0.746$*

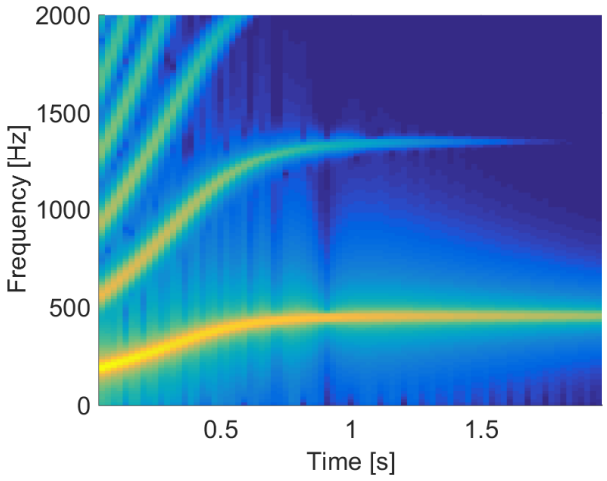

Figure 11: *Spectrogram of the system response x_1 for a control parameter value $\epsilon_2 = 1.791$*

5. CONCLUSION

This paper has introduced a port-Hamiltonian formulation of a *xiaoluo* gong's fundamental nonlinear mode described by a softening Duffing oscillator. First, the calculation of the Duffing energy highlighted an inconsistent potential energy that has led to the redefinition of a well-posed potential energy. Guaranteed-passive simulations of the system associated to this new energy prove to overcome the stability problem encountered with the ill-posed Duffing modelling. The new energy formulation has then been used in successful energy shaping control simulations, in order to modify the system's nonlinear behaviour in a more hardening or more softening way.

This work represents the first step toward the development of an experimental control of a real *xiaoluo* gong. However, the various nonlinear phenomena encountered in gong's dynamics, in particular internal resonances (energy exchanges between modes), underline the limitation of a single nonlinear mode modelisation. The control of the instrument pitch glide may require the identification of a MDOF model with interconnected port-Hamiltonian systems.

6. ACKNOWLEDGMENTS

This work was funded by the PhD grant of Marguerite Jossic (Université Pierre et Marie Curie, France) and the French National Research Agency sponsored project INFIDHEM.

7. REFERENCES

[1] N.H. Fletcher, "Nonlinear frequency shifts in quasispherical-cap shells: Pitch glide in chinese gongs," *The Journal of the Acoustical Society of America*, vol. 78, no. 6, pp. 2069–2073, 1985.

[2] Cyril Touzé M. Ducceschi and S. Bilbao, "Nonlinear vibrations of rectangular plates: Investigation of modal interaction and coupling rules," *Acta Mechanica*, pp. 213–232, 2014.

[3] Thomas D Rossing and NH Fletcher, "Nonlinear vibrations in plates and gongs," *The Journal of the Acoustical Society of America*, vol. 73, no. 1, pp. 345–351, 1983.

[4] N.H. Fletcher and T.D. Rossing, *The Physics of musical instruments*, Springer-Verlag, 1998.

[5] A. Chaigne C. Touzé O. Thomas, "Hardening/softening behaviour in non-linear oscillations of structural systems using non-linear normal modes," *Journal of Sound and Vibration*, pp. 77–101, 2004.

[6] G. Kerschen, M. Peeters, J.C. Golinval, and A.F. Vakakis, "Nonlinear normal modes, part i: A useful framework for the structural dynamicist," *Mechanical Systems and Signal Processing*, vol. 23, no. 1, pp. 170–194, 2009.

[7] C. Touzé M. Ducceschi, O. Cadot and S. Bilbao, "Dynamics of the wave turbulence spectrum in vibrating plates: a numerical investigation using a conservative finite difference scheme," *Physica D*, pp. 73–85, 2014.

[8] S. Bilbao, "A family of conservative finite difference schemes for the dynamical von karman plate equations," *Numerical Methods for Partial Differential Equations*, pp. 193–216, 2008.

[9] Cyril Touzé and M Amabili, "Nonlinear normal modes for damped geometrically nonlinear systems: application to reduced-order modelling of harmonically forced structures," *Journal of sound and vibration*, vol. 298, no. 4, pp. 958–981, 2006.

[10] Ali Hasan Nayfeh and Dean T. Mook, *Nonlinear oscillations*, J. Wiley, 1995.

[11] Simon Peter, Robin Riethmüller, and Remco I. Leine, *Tracking of Backbone Curves of Nonlinear Systems Using Phase-Locked-Loops*, pp. 107–120, Springer International Publishing, Cham, 2016.

[12] A. Falaize and T. Hélie, "Passive guaranteed simulation of analog audio circuits: A port-hamiltonian approach," *Applied Sciences (Balcan Society of Geometers)*, vol. 6, pp. pp.273 – 273, 2016.

[13] N. Lopes, T. Hélie, and A. Falaize, "Explicit second-order accurate method for the passive guaranteed simulation of port-hamiltonian systems," *IFAC-PapersOnLine*, vol. 48, no. 13, pp. 223 – 228, 2015.

[14] V. Duindam, A. Macchelli, S. Stramigioli, and H. Bruyninckx, *Modeling and Control of Complex Physical Systems: The Port-Hamiltonian Approach*, Springer, 2009.

[15] S. Benacchio, B. Chomette, A. Mamou-Mani, and V. Finel, "Mode tuning of a simplified string instrument using time-dimensionless state-derivative control," *Journal of Sound and Vibration*, vol. 334, pp. 178–189, 2015.

[16] Antoine Chaigne, Cyril Touzé, and Olivier Thomas, "Nonlinear vibrations and chaos in gongs and cymbals," *Acoustical science and technology*, vol. 26, no. 5, pp. 403–409, 2005.

[17] Antoine Falaize and Thomas Hélie, "Passive simulation of the nonlinear port-hamiltonian modeling of a rhodes piano," *Journal of Sound and Vibration*, vol. 390, pp. 289 – 309, 2017.

[18] M. Jossic, A. Mamou-Mani, B. Chomette, D. Roze, F. Ollivier, and C Josserand, "Modal active control of chinese gongs," *Journal of the Acoustical Society of America*, 2017, Submitted.

[19] KA Legge and NH Fletcher, "Nonlinearity, chaos, and the sound of shallow gongs," *The Journal of the Acoustical Society of America*, vol. 86, no. 6, pp. 2439–2443, 1989.

[20] T. Meurisse, A. Mamou-Mani, S. Benacchio, B. Chomette, V. Finel, D. B. Sharp, and R. Caussé, "Experimental demonstration of the modification of the resonances of a simplified self-sustained wind instrument through modal active control," *Acta Acustica*, vol. 101, no. 3, pp. 581–593(13), 2015.

[21] J.P. Noel and G. Kerschen, "Nonlinear system identification in structural dynamics: 10 more years of progress," *Mechanical Systems and Signal Processing*, vol. 83, pp. 2–35, 2017.

[22] Andre Preumont, *Vibration control of active structures: an introduction*, vol. 50, Springer Science & Business Media, 2012.